Journal of Applied Spectroscopy, Vol. 74, No. 1, 2007

MODELING THE ATOMIC AND ELECTRONIC STRUCTURE OF DIAMOND NANOCRYSTALS CONTAINING $[NV]^-$ CENTERS BY THE DENSITY FUNCTIONAL METHOD

V. A. Pushkarchuk,[*1] S. Ya. Kilin,[2] A. P. Nizovtsev,[2] A. L. Pushkarchuk,[3] A. B. Filonov,[1] and V. E. Borisenko[1]

UDC 535.33:548.0

We have used the density functional method to model the atomic and electronic structure of diamond nanocrystals passivated by hydrogen atoms and either not containing defects or containing a single [NV]– center. We have shown that in all cases, after relaxation the nanocrystals are formed as diamond-like structures.

We have studied the features of the electronic structure of the nanocrystals. We have analyzed in detail the mechanism for the formation of energy levels in the bandgap due to $[NV]^-$ centers. We have established that the optical absorption and fluorescence spectra for the $[NV]^-$ centers are mainly associated with transitions of electrons between the highest occupied β orbitals (projection of the electron spin equal to +1/2) and lower unoccupied α orbitals (projection of the electron spin equal to –1/2). The results on the localization and energy position of the states in the bandgap match data obtained for the $[NV]^-$ center in bulk diamond.

Key words: *diamond nanocrystals, $[NV]^-$ center, electronic structure, density functional, fluorescence.*

Introduction. In recent years, significant progress has been made in improving the technology for obtaining nanosized diamonds by detonation synthesis and chemical vapor deposition (CVD) (see, for example, [1, 2]), stimulated by the possibilities for broad application of nanodiamonds for making ultrathin, superhard coatings, nanocomposites, abrasive materials and lubricants, sorbents etc. A promising new area of application for nanodiamonds is using them to make cheap widescreen displays [3, 4]. The indicated practical requirements have been why detailed study is needed of the structural, surface, spin, and optical properties of nanodiamonds, which are substantially different from the analogous properties of bulk diamond samples.

While the properties of bulk diamond samples have been well studied in decades of studies by very different methods, including *ab initio* calculations [5–7], such study has still only begun for nanocrystalline diamond [8–12]. In particular, in [9–11] detailed ab initio calculations were performed for the structure, stability, and optical properties of nanosized diamonds. For nanodiamonds whose surface is passivated by hydrogen, in [11] it was demonstrated that quantum size effects are not important for x-ray emission and absorption spectra as the sizes of the nanoclusters decrease all the way down to 1 nm.

Defects present in nanocrystalline diamond have a significant effect on its properties. In particular, substitutional defects (nitrogen, phosphorus, boron, silicon) and their combinations with vacancies create additional levels in the bandgap, and consequently such defects can be considered as isolated quantum systems, the weak coupling of which with the rigid lattice of the surrounding diamond is responsible for their exceptionally high photostability even at room temperature. This is important for practical use of such defects as sources of individual photons for quantum cryptographic systems now actively under development, the principal advantage of which is the impossibility of undetectable interception of transmitted information encoded in the states of individual photons.

One of the most well studied defects in diamond is the nitrogen-vacancy center (NV center), consisting of a substitutional nitrogen atom and a vacancy located on an adjacent lattice point of the diamond lattice. Owing to its op-

[*]To whom correspondence should be addressed.

[1]Belorussian State University of Information Science and Electronics, 6 ul. P. Brovki, Minsk 220013. E-mail: vadim9@gmail.com. [2]B. I. Stepanov Institute of Physics, National Academy of Sciences of Belarus, Minsk. [3]Institute of Physical Organic Chemistry, National Academy of Sciences of Belarus, Minsk. Translated from Zhurnal Prikladnoi Spektroskopii, Vol. 74, No. 1, pp. 86–92, January–February, 2007. Original article submitted August 3, 2006.

0021-9037/07/7401-0095

tical properties (high quantum yield of ~1, the presence of a triplet-triplet optical transition, spin-selective photokinetics), the center has been widely used in quantum optics as a source of individual photons [13–15], a q-bit (qubit) carrier [16, 17], and a light source for near-field spectroscopy [18]. Recently full-scale transfer of a quantum key has been demonstrated through air at night using a quantum cryptographic system in which an individual NV center in nanocrystalline diamond was used as the source of individual photons with subsequent polarization encoding (the BB84 protocol).

NV centers are present both in natural diamonds and in synthetic diamonds. Trapping an electron, the center becomes a negatively charged $[NV]^-$ center, which has a characteristic phononless line in the absorption and fluorescence spectra at a wavelength of ~637 nm (energy 1.935 eV). A spectroscopic feature of the $[NV]^-$ center is that the optical transitions in it occur between the triplet electronic ground state ^3A and the excited triplet electronic state ^3E (S = 1), each of which is split by the diamond crystal field into a series of magnetic sublevels of fine structure with distances between them on the order of a few gigahertz (in the absence of an external magnetic field). Owing to the large oscillator strength of the ^3A–^3E transition and the almost ideal quantum yield, single molecule spectroscopy methods have been used to detect $[NV]^-$ centers as individual quantum objects at room temperatures and helium temperatures. Furthermore, the triplet nature of the ^3A electronic ground state meant that it was possible to study and manipulate in a targeted fashion the pure quantum state of the single electron spin of the center in this state, using optically detected magnetic resonance [18–21]. If there are ^{13}C carbon atoms (nuclear spin I = 1/2) near the $[NV]^-$ center in a diamond lattice, usually consisting of ^{12}C carbon atoms having no nuclear spin, then such a system of interacting electronic and nuclear spins can be used as the prototype for the processor of a quantum computer. Recently, based on the quantum system of a single $[NV]^-$ center + a single ^{13}C nuclear spin in nanocrystalline diamond, a CNOT logic operation was realized at room temperature [20]. The initial quantum state of the system was formed optically, using a laser pulse. The result of the logic operation, executed using pulsed microwave and rf fields, was also counted optically by measuring the fluorescence photons emitted by the center. The results of different types of experiments with single $[NV]^-$ centers in diamond nanocrystals has made it possible to formulate photophysical models for the $[NV]^-$ center and to use them as a basis for describing a broad range of available experimental data [22–24]. Moreover, many questions about the very nontrivial photophysics of the $[NV]^-$ center would be more comprehensible after performing quantum chemical calculations for nanosized diamonds with such centers. To date, calculations have been carried out only for bulk diamond samples [6, 25–27]. In [28–32] the spin properties of such nanostructures were mainly studied. In this paper, we focus special attention on quantum chemical modeling of the spatial and electronic structure of diamond nanocrystals passivated by hydrogen atoms not containing defects or containing $[NV]^-$ centers. These studies are needed for interpretation of the experimental data obtained from the absorption and fluorescence spectra for $[NV]^-$ centers [27].

The Model and the Calculation Method. We have considered diamond nanocrystals for which dangling bonds at the boundaries are passivated by hydrogen atoms. The nanocrystals were constructed based on clusters obtained by separating a group of carbon atoms from the ideal diamond crystal lattice, after which the calculations were performed with the aim of determining the geometric structure of the cluster after relaxation.

The calculations were performed for clusters containing from 17 to 71 carbon atoms. We present the results obtained for a $C_{38}H_{42}$ cluster containing 38 carbon atoms and 42 hydrogen atoms (Fig. 1a), as the most typical for the indicated set of clusters. This cluster belongs to the "BC" (bond-centered) group of clusters, a typical feature of which is the fact that the middle of the cluster is found at the center of a bond between two nearest-neighbor carbon atoms. We chose this cluster as the basic cluster for the following reasons. The cluster diameter is ~1 nm, and the carbon atoms form a tetrahedral diamond-like structure and consequently it belongs to the group of "higher diamondoids" or hydrocarbonates [33, 34]. We know [33] that this group in the structural series of diamond clusters passivated by hydrogen is now of special interest in connection with the prospects for using them as building blocks for automated mechanical synthesis of nanodiamond compounds in nanofactories [34, 35]. The properties of the compounds may be different, but they all have such basic characteristics of natural diamond as a Young's modulus >1050 GPa, melting point >1800^{o}C, density 3500 kg/m^3. Based on these characteristics, we can conclude that any article fabricated from them will have much higher rigidity than an analogous article fabricated from steel, for example; they will have a higher melting point and, owing to the possibility of fabricating fibers, will be much lighter than analogs made from other materials. At the same time, it is specifically this group of nanostructures that has been the least

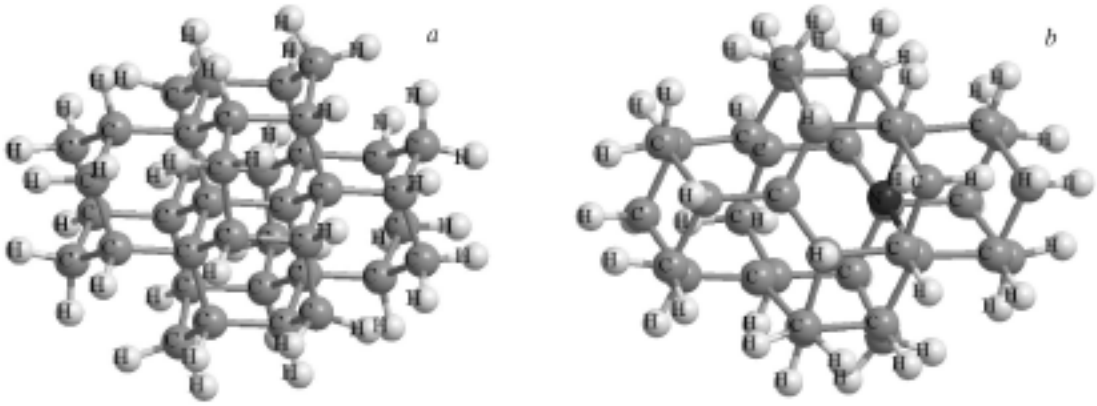

Fig. 1 Graphical representation of $C_{38}H_{42}$ (a) and $C_{36}H_{42}[NV]^-$ (b) clusters.

studied [33], and obtaining more complete information about the atomic structure and the electronic structure for a representative of the indicated class of compounds is certainly of interest.

On the other hand, the atomic configuration of the cluster selected allows us, when considering nanodiamonds containing an $[NV]^-$ center, to take into account its local symmetry in the best way by locating the substitutional nitrogen atom and the vacancy at the center of the cluster at the same distance from its boundary. Accordingly, we can hypothesize that the local symmetry of the immediate environment of this defect after relaxation will qualitatively coincide with relaxation for the analogous defect within the interior of a diamond. This will allow us to make comparisons with available results on the electronic structure of $[NV]^-$ centers within the interior volume that have been obtained by other methods (see, for example, [6, 25–27]).

Based on the $C_{38}H_{42}$ cluster, we generated the cluster $C_{36}H_{42}[NH]^-$ containing an $[NV]^-$ center formed from a divacancy by placing a nitrogen atom in one of the vacant positions (Fig. 1b). In this case, one of the two carbon atoms nearest to the center of the cluster is substituted by the nitrogen atom, while the other is removed from the cluster, forming a vacancy. For the $C_{38}H_{42}$ cluster, the calculations were performed in the singlet ground state ($S = 0$), while for the $C_{36}H_{42}[NV]^-$ cluster, in accordance with much experimental and theoretical [19–27] data, the triplet state ($S = 1$) was taken as the ground state.

From the results of the calculations for the clusters $C_{38}H_{42}$ and $C_{36}H_{42}[NV]^-$, we analyzed their atomic and electronic structure, the localization of the wavefunctions forming the electronic states in the bandgap, and we determined the density of electronic states (DES).

The calculations were carried out with full optimization of the geometric structure of the clusters within the density functional (DF) quantum chemical method, using the B3LYP1 and LSDA functionals and the MINI/6-31G** basis. We used the PC GAMESS software packages, developed based on GAMESS (US) [36, 37].

Discussion of Results. From the results of the calculations, we analyzed the atomic structure of the clusters and the electron density distribution. Here we focused our major attention on the local characteristics in the center of the cluster, where the $[NV]^-$ center will be located. As we see from Fig. 1, the atoms of the clusters form groups belonging to different coordination spheres. For the $C_{38}H_{42}$ cluster, two atoms located at the center of the cluster belong to the first coordination sphere; for $C_{36}H_{42}[NV]^-$, the N atom and a vacancy belong to the first coordination sphere. The second coordination sphere includes the carbon atoms which are nearest neighbors of the atoms in the first coordination sphere. This includes six carbon atoms, where for the $C_{36}H_{42}[NV]^-$ cluster three of them are nearest neighbors of the vacancy, while three are nearest neighbors of the nitrogen atom. A graphical representation and the numbering of the atoms in this group are shown in Fig. 2.

As the basic calculated quantities, we selected: for the $C_{38}H_{42}$ cluster, the distance R_1 between the two C atoms belonging to the first coordination sphere and the distance R_2 between one of the C atoms belonging to the first coordination sphere and one of the C atoms of the second coordination sphere; for the $C_{36}H_{42}[NV]^-$ cluster, the distance R_1 between the N atom and the vacancy and the distance R_2 between the N atom and its nearest neighbor atoms C1, C2, C3 (Fig. 2), belonging to the second coordination sphere, where for all three atoms C1, C2, C3 these dis-

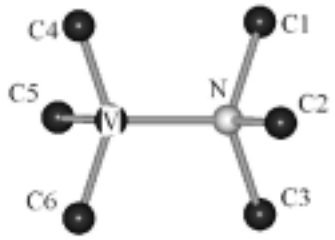

Fig. 2 Groups of atoms included in the first and second coordination sphere of the $C_{36}H_{42}[NV]^-$ cluster.

TABLE 1 Distances (Å) Between C Atoms Belonging to the First Coordination Sphere and Between C Atoms for the $C_{38}H_{42}$ Cluster (R_1) and the C and N Atoms for the $C_{36}H_{42}[NV]^-$ Cluster, Belonging to the First and Second Coordination Sphere (R_2). Electron Density (au) on C Atoms Belonging to the First (ρ_1) and Second (ρ_2) Coordination Sphere for the $C_{38}H_{42}$ Cluster and on the N (ρN) and C (ρC_M) Atoms for the$C_{36}H_{42}[NV]^-$ Cluster

Cluster	R_1	R_2	ρ_1	ρ_2	ρN	ρC_M M = 1–3	ρC_M M = 4–6
$C_{38}H_{42}$	1.61	1.57	0.0	0.01	–	–	–
$C_{36}H_{42}[NV]^-$	1.74	1.49	–	–	–0.25	0.088	–0.03

Note. The numbering of the C atoms corresponds to Fig. 2.

tances are identical and equal to R_2 due to the symmetry of the cluster. We also calculated the electron density on the atoms belonging to the first and second coordination spheres (Table 1).

According to the experimental data in [38], for the crystalline diamond lattice, the C–C distance is 1.541 Å, while there should be no charges on the atoms for a covalent crystal such as diamond. Comparison of the calculation results given in Table 1 with these experimental data for the crystal shows that for the $C_{38}H_{42}$ cluster, the quantities obtained are sufficiently close to those for crystalline diamond (the values of the charges and the bond lengths correspond to covalent single C–C bonds; the atomic structure corresponds to the diamond lattice). Here the bond between the C atoms remains tetrahedral after relaxation. Thus after relaxation, the carbon cluster selected for the study preserves the atomic structure typical of a higher diamondoid [33].

Analysis of the atomic structure calculation results for the $C_{36}H_{42}[NV]^-$ cluster (Table 1) shows that in this case, due to symmetric relaxation, the N atom shifts away from the vacancy along the ⟨111⟩ direction by ≈8% of the length R_1 of the C–C bond in the $C_{38}H_{42}$ cluster, which agrees well with the data in [26, 27] (9% and 8%), in which the calculations were performed for bulk diamond using the model of a supercell containing 54, 128, and 216 atoms. At the same time, the distance R_2(C–N) for the relaxed structure is shortened compared with the length of the C–C bond in diamond and is 1.49 Å, which is 0.05 Å longer and 0.01 Å shorter than the analogous values obtained for this defect in diamond in the cluster approximation [6] (1.44 Å) and in the supercell approximation [25] (1.5 Å), where the direction of relaxation of the C atoms is the same in all cases. The results obtained allow us to conclude that the local symmetry of the $[NV]^-$ center in nanodiamonds after relaxation matches that in bulk structures. At the same time, the typical structure based on tetrahedral covalent bonds for the rest of the $C_{36}H_{42}[NV]^-$ nanocluster is preserved, and as before it can be considered as a diamondoid containing a defect (the $[NV]^-$ center). Analysis of the charge distribution shows that for the case of an $[NV]^-$ center, the excess negative charge is localized on the N atom and on several C atoms located at the boundaries of the cluster. In the central portion of the cluster, the charge distribution does not change significantly compared with the $C_{38}H_{42}$ cluster.

For calculation of the electronic structure of the $C_{38}H_{42}$ nanocluster, we used spin-restricted wavefunctions. We used the calculation results to construct the one-electron levels and the density of states (Fig. 3). From the calculation results it follows that the system under consideration has an electronic structure typical of a semiconductor with

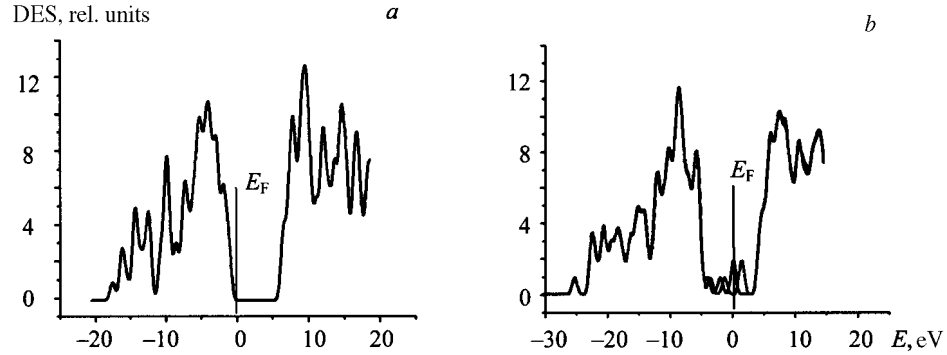

Fig. 3 Density of electronic states (DES) for $C_{38}H_{42}$ (a) and $C_{36}H_{42}[NV]^-$ (b) clusters. Solid line: spin-up energy states (α spin). Dashed line: spin-down energy states (β spin). In all cases, the position of the Fermi level (E_F), which corresponds to the energy position of the HOMO, was taken as the zero for the energy.

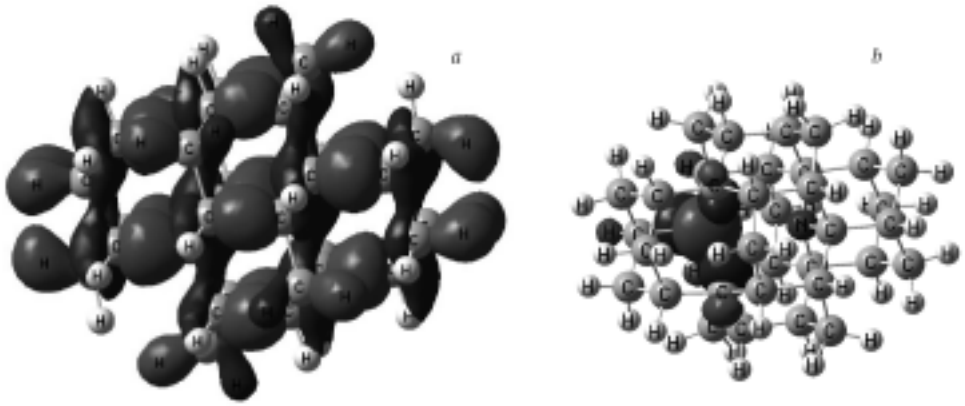

Fig. 4 Localization of the HOMO for the $C_{38}H_{42}$ (a) and $C_{36}H_{42}[NV]^-$ (b) clusters for the density of electronic states given in Fig. 3a and Fig. 3b.

bandgap width E_g = 6.19 eV. The latter value was calculated as the energy difference between energy levels corresponding to the highest occupied molecular orbital (HOMO) and the lowest unoccupied molecular orbital (LUMO). As we see from Fig. 3a, the HOMO corresponding to the valence band edge is localized mainly on the C–C bonds and the H atoms and is uniformly distributed over the entire cluster. Such localization of the valence electrons corresponds to the nature of the localization within bulk diamond, with formation of strong valence bonds, and allows us to conclude that according to these parameters, the considered structure can also be described as a higher diamondoid [33].

In the case of the $C_{36}H_{42}[NV]^-$ nanocluster containing an open electron shell (two unpaired electrons), its electronic structure was calculated using spin-unrestricted wave functions. From the calculation results we constructed the one-electron levels and density of states separately for spin-up (α spin) and spin-down (β spin) states (Fig. 3b). Analysis of the density of states shows that in this case, additional subbands are formed in the bandgap which are formed due to the presence of the $[NV]^-$ center. The lower defect state is found in the region 0.8 eV above the top of the valence band, and the upper defect state is found 2.98 eV below the bottom of the conduction band. Spin splitting of the band increases for states that are higher in energy. In this case, the Fermi level is located in the region 2.6 eV above the top of the valence band and consequently the higher energy spin-down states in the bandgap (β spin) are unoccupied. Such positioning of the states is consistent with the results of calculations performed by the density functional method in the cluster approximation (for a cluster containing ~70 carbon and hydrogen atoms) [6] and in the supercell model [25] for the $[NV]^-$ center in bulk diamond. Analysis of the localization of the HOMO including

a higher energy unpaired electron with spin up (α spin) shows (Fig. 4b) that the wavefunction corresponding to this state is localized on the C4, C5, C6 atoms forming the immediate environment of the vacancy belonging to the $[NV]^-$ center. Thus the optical transitions detected in the absorption and fluorescence spectra are mainly due to electrons populating energy levels which correspond to wavefunctions describing the upper occupied state (α spin). These results are consistent with our calculations on localization of the spin density for analogous structures [28–32] and with the results of [25] for bulk diamond.

Conclusion. For the example of $C_{38}H_{42}$ and $C_{36}H_{42}[NV]^-$ nanoclusters, we have established that the proposed approach gives results close to those obtained in other papers, and allows us to identify the mechanisms for the formation of the characteristic features of the atomic structure and the characteristics of the electronic structure for the studied class of compounds.

We have shown that carbon nanocrystals with dangling bonds at the boundary passivated by hydrogen atoms are formed as diamond-like structures: higher diamondoids in which each C atom is bonded to other atoms via tetrahedral covalent bonds. And in the case when an $[NV]^-$ center is present, the diamond-like structure of the rest of the cluster is preserved, taking into account the slight relaxation of the N atom and the three C atoms closest to the vacancy in the direction away from the center of the defect.

We have established that nanoclusters passivated by hydrogen atoms have an electronic structure typical for semiconductors. It consists of a pronounced valence band and conduction band separated by the bandgap. In this case, the bandgap width for the $C_{38}H_{42}$ nanocluster is ~6.19 eV, which is 0.69 eV greater than the analogous value for bulk diamond and matches known ideas about broadening of E_g for nanoparticles [39].

Nanoclusters containing $[NV]^-$ centers also have an electronic structure typical for semiconductors, but additional sets of states are formed in the bandgap. We have shown that the major role in formation of these defect levels is played by the carbon atoms which are the nearest neighbors of the vacancy of the $[NV]^-$ center, while the surface states are passivated by hydrogen atoms. We have established that the optical spectra are due to transitions of electrons in the highest occupied energy levels, corresponding to wavefunctions describing the α spin state. The results on localization and the energy position of the states in the bandgap match data obtained for the $[NV]^-$ center in bulk diamond [6, 25].

This work was carried out with the partial support of the Belorussian Republic Foundation for Basic Research, INTAS, and the State Comprehensive Program for Scientific Research on Nanomaterials and Nanotechnology.

REFERENCES

1. *Special Issue of Fiz. Tverd. Tela*, **46**, 6–753 (2004).
2. A. Ya. Vul', O. A. Shenderova, and D. M. Gruen, eds., *Synthesis, Properties and Applications of Ultrananocrystalline Diamond*, *NATO Sci. Ser.*, Springer (2005), Vol. 192.
3. W. A. Yarbrough and R. Messier, *Science*, **247**, 688–691 (1990).
4. Y. Lifshitz, Th. Kohler, Th. Frauenheim, I. Guzmann, A. Hoffman, R. Q. Zhang, X. T. Zhu, and S. T. Lee, *Science*, **297**, 1531–1533 (2002).
5. R. P. Messmer and G. D. Watkins, *Phys. Rev. B*, **7**, 2568–2590 (1973).
6. J. P. Goss, R. Jones, S. J. Breuer, P. R. Briddon, and S. Oberg, *Phys. Rev. Lett.*, **77**, 3041–3044 (1996).
7. J. P. Goss, P. R. Briddon, R. Jones, and S. Sque, *J. Phys.: Condens. Matter*, **15**, S2903–S2911 (2003).
8. S. Prawer, K. W. Nugent, D. N. Jamieson, J. O. Orwa, L. A. Bursill, and J. L. Peng, *Chem. Phys. Lett.*, **332**, 93–97 (2000).
9. A. S. Barnard, S. P. Russo, and I. K. Snook, *J. Chem. Phys.*, **118**, 10725–10728 (2003).
10. A. S. Barnard, S. P. Russo, and I. K. Snook, *Int. J. Modern Phys. B*, **17**, 3865–3879 (2003).
11. J.-Y. Raty, G. Galli, C. Bostedt, T. W. van Buuren, and L. J. Terminello, *Phys. Rev. Lett.*, **90**, 037401-1 - 037401-4 (2003).
12. S. Park, D. Srivastava, and K. Cho, J. Nanosci. Nanotech, 1, 75-79 (2001); J. Twamley, *quant-ph/0210202*.
13. C. Kurtseifer, S. Mayer, P. Zarda, and H. Weinfurter, *Phys. Rev. Lett.*, **85**, 290–293 (2000).
14. F. Treussart, R. Alleaume, V. Le Floc'h, L. T. Xiao, J.-M. Courty, and J.-F. Roch, *Phys. Rev. Lett.*, **89**, 093601-1-093601-4 (2002).

15. R. Alleaume, F. Treussart, G. Messin, Y. Dumeige, J.-F. Roch, A. Beveratos, R. Brouri-Tualla, J.-P. Poizat, and P. Grangier, *New J. Phys*., **6**, 1–14 (2004).
16. J. Wrachtrup, S. Ya. Kilin, and A. P. Nizovtsev, *Opt. i Spektr*., **91**, 459–466 (2001).
17. F. T. Charnock and T. A. Kennedy, *Phys. Rev. B*, **64**, 041201-041204 (2001).
18. S. Kuhn, C. Hettich, C. Schmitt, J.-Ph. Poizat, and V. Sandoghdar, *J. Microscopy*, **202**, 2–6 (2001).
19. F. Jelezko, T. Gaebal, I. Popa, A. Gruber, and J. Wrachtrup, *Phys. Rev. Lett*., **92**, 076401-1-076401-4 (2004).
20. F. Jelezko, T. Gaebal, I. Popa, M. Domhan, A. Gruber, and J. Wrachtrup, *Phys. Rev. Lett.*, **93**, 130501-1-130501-4 (2004).
21. F. Jelezko and J. Wrachtrup, *J. Phys.: Condens. Matter*, **16**, R1089-R1104 (2004).
22. A. P. Nizovtsev, S. Ya. Kilin, C. Tietz, F. Jelezko, and J. Wrachtrup, *Physica B*, **308–309**, 608–611 (2001).
23. A. P. Nizovtsev, S. Ya. Kilin, F. Jelezko, I. Popa, A. Gruber, C. Tietz, and J. Wrachtrup, *Opt. i Spektr*., **4**, 848–858 (2003).
24. A. P. Nizovtsev, S. Ya. Kilin, F. Jelezko, I. Popa, A. Gruber, and J. Wrachtrup, *Physica B*, 340–342, 106–110 (2003).
25. M. Luszchek, R. Laskowski, and P. Horodecki, *Physica B*, **348**, 292–298 (2004).
26. A. Mainwood, *Phys. Rev. B*, **49**, 7934–7941 (1994).
27. S. Papagiannidis, "*Ab initio* modeling of defect complexes in semiconductors," Thesis for the academic degree of Doctor of Philosophy (2003).
28. V. A. Pushkarchuk, A. L. Pushkarchuk, S. Ya. Kilin, A. P. Nizovcev, V. E. Borisenko, and A. B. Filonov, in: *Abstracts, Tenth International Conference on Quantum Optics*, 30 May-3 June 2004, Minsk (2004), p. 34.
29. V. E. Borisenko, S. Ya. Kilin, A. P. Nizovtsev, A. B. Filonov, A. L. Pushkarchuk, and V. A. Pushkarchuk, *Izv. Bel. Inzhenern. Akad*., 4, 8–10 (2003).
30. V. A. Pushkarchuk, S. Ya. Kilin, A. P. Nizovtsev, A. L. Pushkarchuk, V. E. Borisenko, C. von Borczyskowski, and A. B. Filonov, *Opt. i Spektr*., **99**, 245–256 (2005).
31. V. A. Pushkarchuk, S. Ya. Kilin, A. P. Nizovtsev, A. L. Pushkarchuk, V. E. Borisenko, C. von Borczyskowski, and A. B. Filonov, in: V. E. Borisenko, S. V. Gaponenko, and V. S. Gurin, eds., *Physics, Chemistry and Application of Nanostructures*, World Scientific (2005), pp. 311–314.
32. V. A. Pushkarchuk, S. Ya. Kilin, A. P. Nizovtsev, V. E. Borisenko, A. B. Filonov, A. L. Pushkarchuk, S. A. Kuten, and C. von Borczyskowski, in: *Abstracts, Eleventh International Conference on Quantum Optics*, 26–31 May 2006, Minsk (2006), pp. 27–28.
33. R. S. Lewis, M. Tang, J. F. Wecker, E. Anders, and E. Steel, *Nature (London)*, **326**, 160–162 (1987).
34. C. Phoenix, *J. Evolution and Technology*, **13**, 1–84 (2003).
35. J. E. Dahl, S. G. Liu, and R. M. K. Carlson, *Science*, **299**, 96–99 (2003).
36. A. Granovsky, http://classic.chem.msu.su/gran/gamess/index.html.
37. M. W. Schmidt, K. K. Baldridge, J. A. Boatz, S. T. Elbert, M. S. Gordon, J. H. Jensen, S. Koseki, N. Matsunaga, K. A. Nguyen, S. Su, T. L. Windus, M. Dupuis, and J. A. Montgomery, *J. Comput. Chem*., **14**, 1347–1351 (1993).
38. E. Cartmell and G. W. A. Fowles, Valency and Molecular Structure [Russian translation], Khimiya, Moscow (1979). [E. Cartmell and G. W. A. Fowles, *Valency and Molecular Structure*, Butterworth (1977).]
39. Y. K. Chang, H. H. Hsieh, W. F. Pong, M.-H. Tsai, F. Z. Chien, P. K. Tseng, L. C. Chen, T. Y. Wang, K. H. Chen, D. M. Bhusari, J. R. Yang, and S. T. Lin, *Phys. Rev. Lett.*, **82**, 5377–5380 (1999).